A general strategy for C(sp^3)–H functionalization with nucleophiles using methyl radical as a hydrogen atom abstractor

Isabelle Nathalie-Marie Leibler,‡ Makeda A. Tekle-Smith,‡ and Abigail G. Doyle

Department of Chemistry, Princeton University, Princeton, New Jersey 08544, United States

The development of general strategies for C(sp^3)–H functionalization is critical to the advancement of modern methods for molecular diversification. In recent years, photoredox catalysis has provided many approaches to C(sp^3)–H functionalization that enable selective oxidation and C(sp^3)–C bond formation via the intermediacy of a carbon-centered radical. While highly enabling, functionalization of the carbon-centered radical is largely mediated by electrophilic reagents, many of which require multi-step preparation and feature low functional group tolerance. By contrast, nucleophilic reagents represent an abundant and practical reagent class. However, few strategies for nucleophilic C(sp^3)–H functionalization from carbon-centered radicals have been identified and existing methodologies either require strong stoichiometric oxidants or are not general for diverse nucleophile incorporation. Here we describe a strategy that transforms C(sp^3)–H bonds into carbocations via sequential hydrogen atom transfer (HAT) and oxidative radical-polar crossover, effecting formal hydride abstraction in the absence of a strong Lewis acid or strong oxidant. The resulting carbocation can be functionalized by a variety of nucleophiles—including halides, water, alcohols, thiols, an electron-rich arene, and an azide—to affect diverse bond formations. Reaction development is demonstrated in the context of nucleophilic fluorination of secondary and tertiary benzylic and allylic C(sp^3)–H bonds and is applicable to late-stage diversification of bioactive molecules. Mechanistic studies indicate that HAT is mediated by methyl radical, a previously unexplored HAT agent

with complementary polarity to those used in photoredox catalysis. Accordingly, this method can deliver unique site-selectivity for late-stage C(sp^3)–H functionalization, as illustrated for the fluorination of ibuprofen ethyl ester.

Catalytic methods for C(sp^3)–H functionalization are of broad value for the construction of synthetic building blocks from feedstock chemicals and for the late-stage derivatization of complex molecules.[1,2] While significant progress has been made in this area, interfacing the cleavage of strong bonds with diverse and useful functionalization remains an outstanding challenge. Chemists have identified multiple strategies for C(sp^3)–H bond cleavage: oxidative addition with a transition metal, concerted C(sp^3)–H insertion, heterolytic cleavage via deprotonation or hydride abstraction, and homolytic cleavage via hydrogen atom transfer (HAT) (**Figure 1A**).[3–9] Among these tactics, hydride abstraction has seen limited development as a result of the requirement for exceptionally strong Lewis acids, which are often incompatible with desirable substrates and functionalization reagents.[6] Nevertheless, access to a carbocation from a C(sp^3)–H bond represents a valuable disconnection due to the versatility of the functionalization step, which can be general for a variety of heteroatom and carbon-centered nucleophiles in their native state.

In contrast to hydride abstraction, HAT can offer a mild and versatile approach to C(sp^3)–H cleavage through the conversion of C(sp^3)–H bonds to radical intermediates.[8,10] While strategies for the homolytic cleavage of C(sp^3)–H bonds have been highly enabling, radical functionalization in these methodologies is primarily restricted to electrophilic reagents (e.g., Selectfluor for fluorination, peroxides for alkoxylation, azodicarboxylates for amination, and electron-deficient arenes for C–C bond formation) (**Figure 1B**).[11–15] Electrophilic reagents are often strong oxidants, expensive to purchase, or require multi-step synthesis, posing significant limitations to their use.[16,17] Whereas nucleophilic reagents represent an abundant and practical reagent class, few

strategies have been reported for radical-based C(sp^3)–H functionalization with nucleophiles.[4,7,18–20] This deficit likely reflects the challenge of productively engaging a nucleophilic carbon-centered radical with a nucleophilic functionalizing reagent.[21]

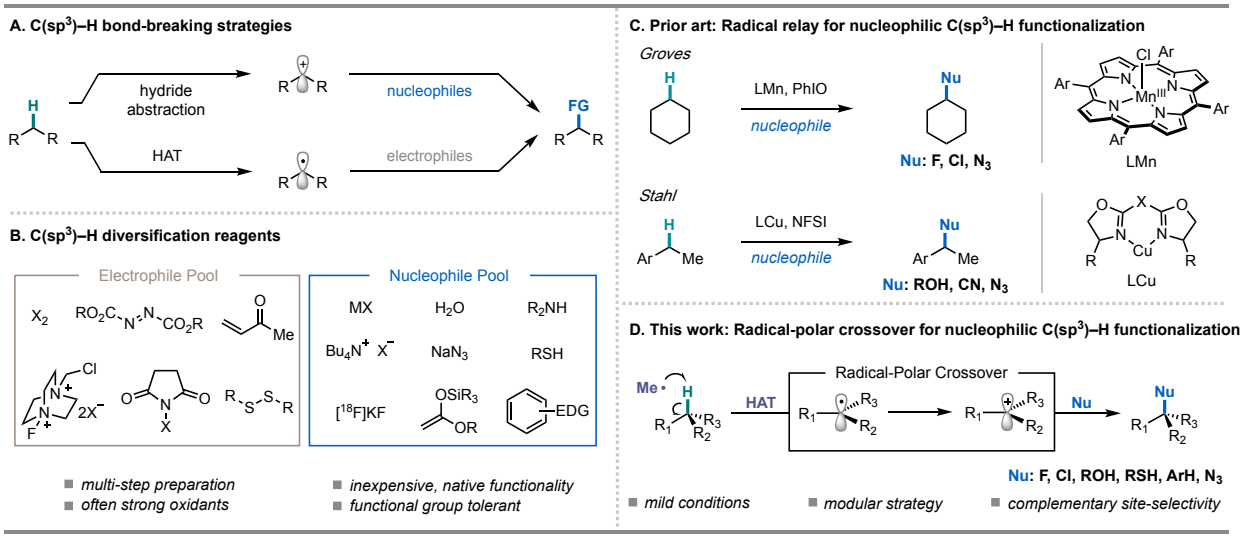

Figure 1. (A) Current mechanisms employed for C(sp^3)–H activation and subsequent functionalization. (B) Array of common electrophilic and nucleophilic functionalizing reagents. (C) Recent examples of nucleophilic C(sp^3)–H functionalization.[22–28] (D) This work. HAT = hydrogen atom transfer.

Recent contributions have centered on the use of a transition-metal catalyst to mediate radical capture and bond formation, rendering the nucleophile an electrophilic ligand in the presence of a stoichiometric oxidant. For example, Stahl and coworkers have demonstrated the utility of copper-catalysis for several nucleophilic C(sp^3)–H functionalization methods, including C(sp^3)–H etherification, cyanation, and azidation (**Figure 1C**).[22–24] Additionally, seminal work from Groves and coworkers has provided strategies for nucleophilic C(sp^3)–H halogenation and azidation using a bioinspired Mn porphyrin catalyst (**Figure 1C**).[25–28] Zhang and coworkers have also developed a fluorination of C(sp^3)–H bonds using a Cu^{III} fluoride complex generated *in situ* from fluoride.[29] While highly enabling, the requirement for strong or super-stoichiometric oxidants in these methods limits their application in synthesis and generality across diverse nucleophile coupling

partners.[19] Thus, the identification of mechanistically distinct strategies for the application of nucleophilic coupling partners could advance the scope and practicality of C(sp^3)–H functionalization methods in chemical synthesis.

Recently, we disclosed a photocatalytic strategy for the decarboxylative nucleophilic fluorination of redox-active esters.[30] This methodology leveraged *N*-acyloxyphthalimides as alkyl radical precursors and an oxidative radical-polar crossover (ORPC) mechanism for the generation of a carbocation poised for nucleophilic addition.[31] Seeking to develop a modular nucleophilic C(sp^3)–H functionalization without the requirement for strong oxidants, we questioned whether photocatalytic ORPC could be combined with principles of HAT to achieve formal hydride abstraction from C(sp^3)–H bonds. Given the versatility of carbocation intermediates, such a reaction platform could provide a general route to numerous desirable transformations such as C(sp^3)–H halogenation, hydroxylation, and C–C bond formation by combining two abundant and structurally diverse feedstocks. While access to carbocation intermediates may be accomplished electrochemically, contemporary methodologies are largely limited by the high overpotential required for reactivity, thereby restricting the scope of amenable C(sp^3)–H and nucleophile coupling partners.[32,33] Whereas C(sp^3)–H functionalization via HAT-ORPC has been proposed in a recent study from Liu and Chen, the method uses a strong, stoichiometric oxidant and solvent quantities of nucleophile.[7] Here we report a HAT-ORPC platform for C(sp^3)–H functionalization using a mild, commercially available *N*-acyloxyphthalimide as HAT precursor. The platform enables C(sp^3)–H fluorination of secondary and tertiary benzylic and allylic substrates using Et_3N•3HF. Additionally, we demonstrate the versatility of the reaction platform to achieve C(sp^3)–H chlorination, hydroxylation, etherification, thioetherification, azidation, and carbon–carbon bond formation.

Our initial investigations focused on C(sp^3)–H fluorination, a valuable transformation in organic synthesis due to the unique chemical properties conferred by fluorine substitution.[34,35] Few reports detailing C(sp^3)–H fluorination with fluoride have been disclosed, due not only to the broad challenges posed by C(sp^3)–H activation, but also the attenuated nucleophilicity of fluoride.[18,25,29,36–38] Despite these challenges, the development of nucleophilic C(sp^3)–H fluorination methods is desirable given the low cost of fluoride sources and their application to radiofluorination for positron emission tomography (PET) imaging.[35]

To evaluate the feasibility of the HAT-ORPC strategy for C(sp^3)–H fluorination, we investigated the conversion of diphenylmethane to fluorodiphenylmethane **2** using a variety of phthalimide-derived HAT precursors (**Table 1**). We focused on *N*-acyloxyphthalimides and *N*-alkoxyphthalimides, as these redox-active species deliver a radical HAT agent via reductive fragmentation, leaving an oxidized photocatalyst available to execute ORPC; furthermore, these reagents are easy to prepare and tune, and are less oxidizing than the stoichiometric oxidants used in radical relay strategies.[39] Optimization of the HAT precursor focused on three design elements: **1)** redox compatibility, **2)** bond dissociation energy (BDE) of the radical generated upon fragmentation (favorable thermodynamics), and **3)** nucleophilicity of the HAT byproduct (competitive carbocation functionalization). We were pleased to find that using Ir(*p*-F-ppy)$_3$ as a photocatalyst, Et_3N•3HF as a fluoride source, and HAT abstractor **3** (MeO–H BDE = 105 kcal/mol) in pivalonitrile afforded alkyl fluoride **2** in 45% yield (**Table 1**, **entry 1**).[40,41] In addition to desired fluoride **2**, we observed generation of the corresponding benzhydryl methyl ether in 7%

yield, resulting from competitive trapping of the carbocation with methanol. Moreover, analysis of the reaction mixture indicated poor conversion of **3**, possibly arising from inefficient single-electron reduction and fragmentation of the *N*-alkoxyphthalimide ($E_{1/2}^{red} \sim -1.42$ V vs. SCE).[42]

These observations prompted us to evaluate *N*-acyloxyphthalimide **4** ($E_{1/2}^{red} \sim -1.2$-1.3 V vs. SCE), a benzoyloxy radical precursor.[42] Upon HAT, this radical generates benzoic acid, a less nucleophilic byproduct than methanol. However, **4** did not improve the reaction yield (**Table 1, entry 2**), likely due to competitive generation of the insufficiently reactive phthalimide radical upon SET and fragmentation (phthalimide N–H BDE = 89.1 kcal/mol vs. benzoic acid O–H BDE = 111 kcal/mol).[43] Instead, we found that *N*-acyloxyphthalimide **1** —a methyl radical precursor— was the most effective HAT reagent, delivering the desired fluoride **2** in 88% yield (**Table 1**, **entry 3**). Abstractor **1** is likely effective because there is a strong thermodynamic and entropic driving force associated with formation of methane (BDE = 105 kcal/mol), an inert, non-nucleophilic byproduct.[40] Notably, **1** is

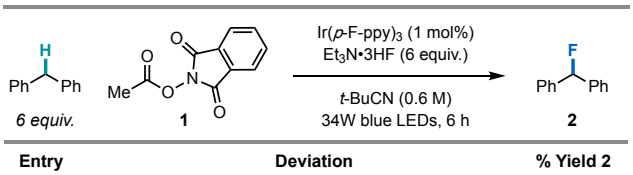

Entry	Deviation	% Yield 2
1[a]	abstractor **3**	**45** (7)
2	abstractor **4**	**20**
3	none	**88**
4	abstractor **5**	**3**
5	**[Ir(dF-CF$_3$-ppy)$_2$(dtbpy)]PF$_6$** instead of **Ir(*p*-F-ppy)$_3$**	**21**
6	**Ir(ppy)$_3$** instead of **Ir(*p*-F-ppy)$_3$**	**43**
7	MeCN instead of *t*-BuCN	**25**
8	CH_2Cl_2 instead of *t*-BuCN	**44**
9	3 equiv. diphenylmethane	**53**
10	1 equiv. diphenylmethane	**17**
11[b]	without abstractor, without photocatalyst, without light	**0**

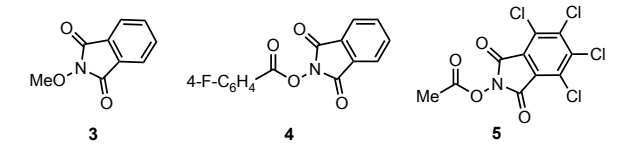

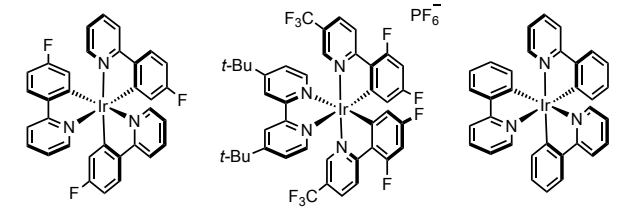

Table 1. Reactions performed on 0.15 mmol scale with 1-fluoronaphthalene added as an external standard (^{19}F NMR yield). *t*-BuCN = pivalonitrile. All potentials given are versus a saturated calomel electrode (SCE) and taken from ref. 46. [a]Parentheses indicate yield of the benzhydryl methyl ether product (^{1}H NMR yield). [b]Each control reaction was completed independently in the absence of key reaction components.

commercially available and can also be prepared on multi-decagram scale in one step from low-cost, readily available materials.[44] Tetrachlorophthalimide analogue **5** was also investigated, but the poor solubility of **5** led to trace conversion (**Table 1**, **entry 4**).[45] With **1**, Ir(*p*-F-ppy)$_3$ was the optimal photocatalyst for this transformation, presumably because Ir(*p*-F-ppy)$_3$ allows for both the reductive generation of methyl radical ($^*Ir^{III}/Ir^{IV}$ $E_{1/2}$ = -1.9 V vs. SCE for Ir(*p*-F-ppy)$_3$ and $E_{1/2}^{red}$ = -1.24 V vs. SCE for **1**) and the oxidation of diphenylmethyl radical (Ir^{IV}/Ir^{III} $E_{1/2}$ = 0.96 V vs. SCE and $E_{1/2}^{ox}$ = 0.35 V vs. SCE for 2° benzylic).[42,46,47] Use of either less reducing or less oxidizing photocatalysts resulted in diminished yields (**Table 1**, **entries 5-6**). While highest yields were observed with 6 equivalents of the C(sp^3)–H partner, 3 equivalents and 1 equivalent of the substrate could also be used, albeit with diminished reactivity (53% and 17% yield respectively) (**Table 1**, **entry 9 and 10**). Finally, control reactions indicate that HAT reagent **1**, photocatalyst, and light are all necessary for reactivity (**Table 1**, **entry 11**).

With optimized conditions established, we set out to examine the scope of C(sp^3)–H fluorination (**Figure 2**). Notably, benzhydryl C(sp^3)–H partners supplied fluorinated products in good to excellent yield (**2**, **6-10**). *ortho*-Substitution was also tolerated (**9**). For substrates possessing both primary and secondary benzylic C(sp^3)–H bonds (**8-10**), excellent regioselectivity was observed for secondary benzylic fluorination (e.g., 10:1 2°:1° for **8**, >20:1 2°:1° for **9** and **10**). Next, a series of electronically diverse ethylbenzene derivatives were examined. A broad range of functional group handles, including halogen (**16-18**), ether (**11** and **12**), carbonyl (**19** and **20**), nitrile (**22**), and trifluoromethyl (**21**) substituents, afforded the corresponding fluorinated products. Electron-rich functionality, traditionally vulnerable to electrophilic reagents or stoichiometric oxidants, was well tolerated (**11** and **12**).[48,49] In general, electron-rich ethylbenzenes displayed higher reactivity (**11-13** and **15**) than more electron-deficient analogues (**19-22**). This trend is

consistent with electron donating substituents conferring higher carbocation stability than electron withdrawing analogues. For substrates possessing multiple secondary benzylic C(sp^3)–H bonds, selective monofluorination was observed (**23-25**). The geometric constraints inherent to the frameworks of acenaphthene and 9H-fluorene resulted in diminished yields, suggesting that carbocation planarity and stabilizing hyperconjugation effects are advantageous structural characteristics (**25** and **26**).[50]

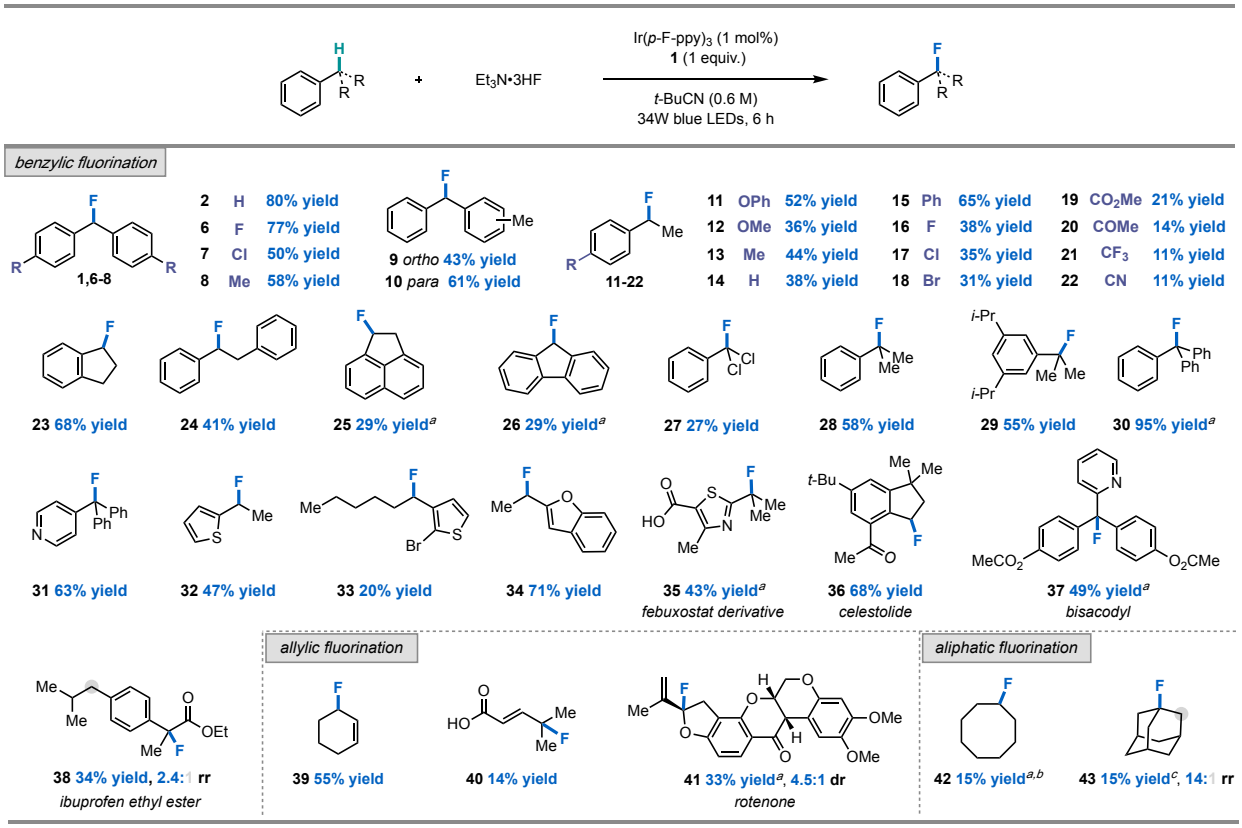

Figure 2. Scope of C(sp^3)–H fluorination (0.25 mmol scale, 6.0 equiv. C(sp^3)–H coupling partner, 6.0 equiv. Et_3N•3HF, ^{19}F NMR yields). [a] 3.0 equiv. C(sp^3)–H coupling partner. [b] Reaction performed with 20 mol % *n*-Bu_4NPF_6. [c] Reaction performed using Ir(*p*-CF_3-ppy)$_3$ as photocatalyst, 1,2-difluorobenzene as solvent, and abstractor **3**.

Tertiary benzylic C(sp^3)–H partners underwent functionalization to generate fluorinated products often inaccessible via nucleophilic fluorination due to slow substitution and competitive elimination (**28, 29, and 35**).[51] Fluorination of benzal chloride yielded a tetra-substituted center with mixed multi-halogenation (**27**). Moreover, fluorination of triphenylmethane proceeded in

95% yield from only 3 equiv. of the C(sp^3)–H coupling partner (**30**). Notably, 4-pyridyl diphenylmethane underwent fluorination in 63% yield, demonstrating tolerance to a valuable *N*-heterocycle scaffold (**31**).[52] Other heterocycles such as thiophenes, furans, and thiazoles were also tolerated under the reaction conditions (**32-35**). Since many bioactive compounds contain heterocyclic fragments, this observation prompted us to evaluate the method for the late-stage derivatization of various pharmaceuticals and complex molecules. Gratifyingly, commercially available bioactive molecules such as a febuxostat derivative, celestolide, bisacodyl, and ibuprofen ethyl ester gave the corresponding fluorinated products in 43%, 68%, 49%, and 34% yield, respectively (**35-38**).

Nucleophilic fluorination could also be extended to allylic C(sp^3)–H coupling partners. Allylic fluorides are valuable motifs in medicinal chemistry and are useful building blocks in synthesis.[53] The development of allylic C(sp^3)–H fluorination methods has proven challenging, as most electrophilic reagents and stoichiometric oxidants utilized in fluorination methodologies favor olefin oxidation over C(sp^3)–H functionalization; alternatively most sources of fluoride facilitate competitive elimination.[29,37,54,55] As an illustration of the mildness of a HAT-ORPC strategy, the fluorination of cyclohexene proceeded in 55% yield (**39**), a significant improvement to our prior efforts in the allylic C(sp^3)–H fluorination of this substrate using a Pd/Cr cocatalyst system.[37] Furthermore, the fluorination of 4-methyl-2-pentenoic acid and the pesticide rotenone occurred in 14% and 33% yield, respectively (**40** and **41**). Finally, as a proof of concept, the unactivated C(sp^3)–H scaffolds of cyclooctane and adamantane underwent fluorination to deliver **42** and **43** in low yield.

Difluoromethylene units have emerged as important lipophilic bioisosteres of hydroxyl and thiol functional groups in drug design.[56] Deoxyfluorination with (diethylamino)sulfur trifluoride (DAST) and pre-oxidized ketones is typically used to install this group.[57] However, given the handling difficulties associated with DAST and its tendency to promote elimination, novel strategies for difluoromethylation are in high demand. We envisioned that benzylic fluorides generated *in situ* from their monochlorinated precursors could deliver difluorinated products under optimized C(sp^3)–H fluorination conditions. To our delight, difluorinated products **44** and **45** were obtained in 63% and 29% yield from the corresponding benzyl chloride (**Figure 3**). To our knowledge, this represents the first nucleophilic C(sp^3)–H fluorination to achieve difluorinated motifs. Notably, difunctionalization is not observed to an appreciable extent in the fluorination of $ArCH_2R$ precursors, even though HAT with the mono-fluorinated product is favorable on account of weaker BDFEs and polarity matching (methyl radical is mildly nucleophilic).[58] We hypothesize that monofluorination selectivity results from the relative stoichiometry of starting material and abstractor, which likely serves to mitigate unproductive side-reactivity involving methyl radical.[59]

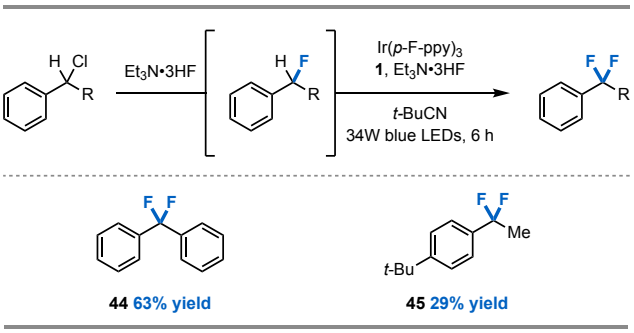

Figure 3. Scope of C(sp^3)–H difluorination (0.25 mmol scale, ^{19}F NMR yield). See SI for reaction details.

Next, we evaluated whether this strategy could serve as a platform for C(sp^3)–H functionalization with other nucleophiles (**Figure 4**). Indeed, we were pleased to find that only minor adjustments to the standard fluorination conditions were needed to accommodate nucleophiles other than Et_3N•3HF. Irradiation of 4,4′-difluorodiphenylmethane with 1 mol % Ir(*p*-F-ppy)$_3$, 15 mol % Et_3N•3HF, HAT precursor **1**, and 6 equiv. of water in pivalonitrile afforded

benzhydryl alcohol **46** in 36% yield (*vide infra*). Hydroxylation took place with no evidence of overoxidation to the ketone in the synthesis of both **46** and **47**, a common limitation of many C(sp^3)–H oxidation methods.[60] These conditions were also amenable to the hydroxylation of a tertiary C(sp^3)–H substrate (**57**). Furthermore, nucleophiles such as methanol and methanol-d_4 afforded methyl ether products **48** and **49** in 40% and 42% yield, respectively. More complex oxygen-centered nucleophiles, including a 1,3-diol and dec-9-en-1-ol, were also compatible (**52** and **53**). Furthermore, we were pleased to accomplish the installation of a C(sp^3)–Cl bond using HCl•Et_2O as a nucleophile[61] (**50**), and to discover that C(sp^3)–N bond formation could be achieved through cross coupling with azidotrimethylsilane (**51**). The construction of medicinally valuable thioethers was also possible, using cyclohexanethiol (**54**) and methylthioglycolate (**55**) as sulfur-based nucleophiles. In particular, the implementation of sulfur nucleophiles highlights the mildness of reaction conditions, as thiol oxidation could otherwise interfere with C(sp^3)–S bond formation under alternative C(sp^3)–H functionalization approaches. Finally, carbon–carbon bond formation via a mild, direct Friedel-Crafts alkylation was accomplished in 41% yield from the coupling of 1,3,5-trimethoxybenzene and 4,4′-difluorodiphenylmethane (**56**). Friedel-Crafts reactions typically require pre-oxidized substrates—such as alkyl halides—and Lewis or Brønsted acid conditions that are often incompatible with the desired nucleophiles.[62,63]

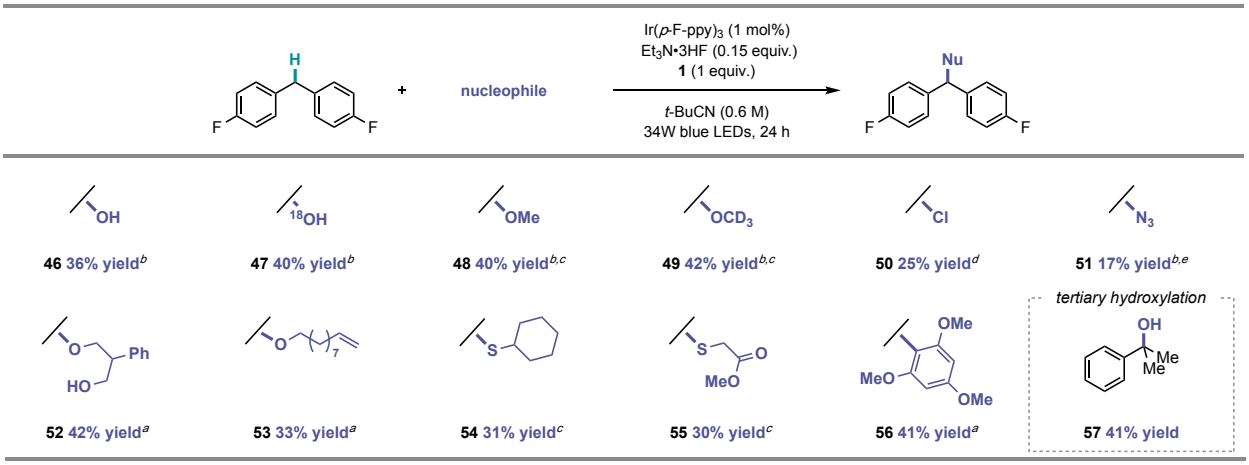

Figure 4. Scope of general nucleophilic C(sp^3)–H functionalization (0.25 mmol, 6.0 equiv. C(sp^3)–H coupling partner, 6.0 equiv. nucleophile, isolated yields). [a] 3.0 equiv. nucleophile. [b] ^{19}F NMR yield. [c] 6 hour reaction. [d] Reaction was performed without $Et_3N•3HF$. [e] Reaction was performed without $Et_3N•3HF$ and with 0.15 equiv. H_2O.

Having evaluated the scope of this transformation, we set out to interrogate its mechanism (**Figure 5**). According to our prior studies[30] and literature precedent[64], we propose that visible light irradiation of the photocatalyst Ir(*p*-F-ppy)$_3$ generates a long-lived excited state that serves as a single-electron reductant of **1**. Fragmentation of the resulting radical anion followed by extrusion of CO_2 forms phthalimide anion and methyl radical. Since methyl radical is thermodynamically disfavored to undergo oxidation by Ir^{IV}, it is instead available to facilitate HAT with the C(sp^3)–H coupling partner to deliver a carbon-centered radical and methane as a byproduct ($E_{1/2}^{ox}$ ~2.5 V vs. SCE for methyl radical). Oxidative radical-polar crossover between Ir^{IV} and the substrate radical generates a carbocation and turns over the photocatalyst. Subsequent nucleophilic trapping of the carbocation intermediate furnishes the desired product (**Figure 5A**).

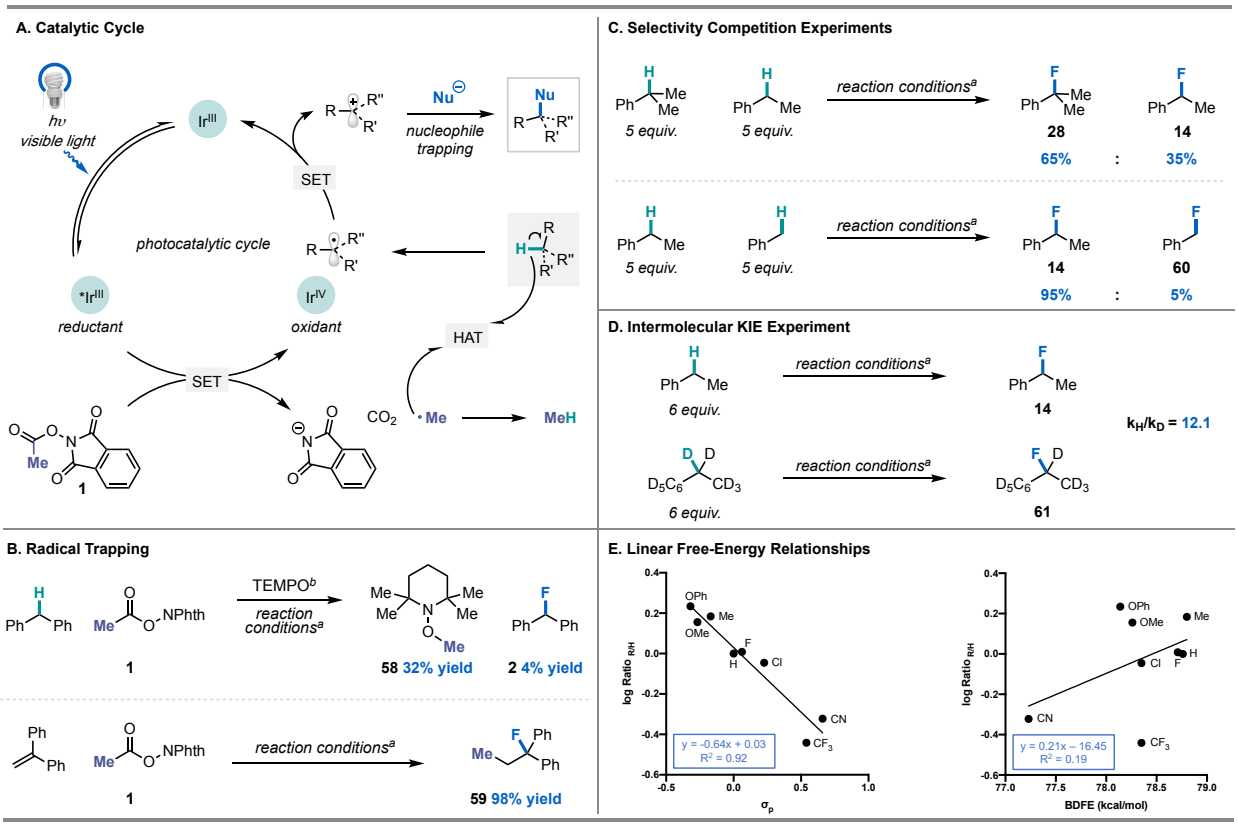

Figure 5. (A) Proposed catalytic cycle. (B) Radical trapping experiments. (C) Investigation of regioselectivity via competition experiments among 3°, 2° and 1° C(sp^3)–H coupling partners. (D) Investigation of kinetic isotope effect *via* parallel initial rates experiment with ethylbenzene and ethylbenzene-d_{10}. (E) Hammett analysis and correlation of selectivity with computed BDFE for a series of ethylbenzene derivatives (See SI). [a] For reaction conditions see **Figure 2** (^{19}F NMR yields). [b] Reaction performed with 1.5 equiv. TEMPO (^{1}H NMR yield).

Consistent with the proposed first step of this mechanism, emission quenching experiments demonstrated that **1** is the only reaction component that quenches the excited state of the photocatalyst (See SI). Our analysis also indicates that the rate of quenching is moderately enhanced in the presence of Et_3N•3HF. This observation is consistent with the higher yields observed when Et_3N•3HF is employed as a catalytic additive for the construction of C(sp^3)–O, C(sp^3)–S, and C(sp^3)–C bonds. The presence of an acidic additive could aid reduction of **1** via proton-coupled electron transfer, as reported for related systems in the literature.[65] In addition, the additive could prevent back-electron transfer and aid fragmentation of the reduced *N*-acyloxyphthalimide **1**.

Next, radical trapping experiments were conducted to evaluate the identity of key radical intermediates in the proposed mechanism. When the fluorination of diphenylmethane was conducted under standard conditions in the presence of 1.5 equiv. of TEMPO, we observed the methyl radical–TEMPO adduct (**58**) in 32% yield, accompanied by nearly complete suppression of fluorination (**Figure 5B**). Additionally, when 1,1-diphenylethylene was employed as a substrate under standard conditions, nearly quantitative carbofluorination was observed, wherein methyl radical addition into the olefin followed by radical oxidation and nucleophilic fluorination delivered product **59**. (**Figure 5B**). This example of carbofluorination not only provides clear evidence for methyl radical formation, but also serves as a useful framework for sequential C(sp^3)–C(sp^3) and C(sp^3)–F alkene difunctionalization. As further evidence, *in situ* NMR studies revealed evolution of methane gas as the reaction proceeded, supporting the involvement of methyl radical in HAT (**Figure S25**).

To our knowledge, methyl radical guided HAT has not been previously explored for photocatalytic C(sp^3)–H functionalization. As such, we set out to understand the reactivity and selectivity effects inherent to the system. We conducted a series of competition experiments with cumene, ethylbenzene, and toluene under standard C(sp^3)–H fluorination conditions (**Figure 5C**). We found that HAT mediated by methyl radical and subsequent ORPC is preferential for 3°>2°>1° benzylic C(sp^3)–H bonds. The data suggest that steric or polarity effects associated with HAT from a mildly nucleophilic methyl radical are minimal in these systems. Instead, the observed site-selectivity is consistent with the relative BDFEs and radical oxidation potential of the tertiary, secondary, and primary substrates.

To probe the independent roles of HAT and radical oxidation, we first conducted a kinetic isotope effect (KIE) study with ethylbenzene. A KIE of 12.1 was measured via parallel initial rate

287 experiments using ethylbenzene and ethylbenzene-d_{10} (**Figure 5D**). The magnitude of the KIE is
288 consistent with prior studies of HAT involving methyl radical and suggests that HAT is the
289 turnover-limiting step.[66,67] To probe the effect of electronics on a HAT-ORPC mechanism, a
290 Hammett analysis of the relative rate of benzylic fluorination across a series of *para*-substituted
291 ethylbenzenes (determined by competition experiments, see SI) was performed (**Figure 5E**).
292 Given the mild nucleophilicity of methyl radical, we might expect electron-deficient ethylbenzenes
293 to undergo fluorination at a faster rate than electron-rich ethylbenzenes. However, the measured ρ
294 value of -0.64 ± 0.07 (R^2 = 0.92) indicates that electron-rich ethylbenzenes undergo C(sp^3)–H
295 fluorination more favorably than electron-deficient derivatives. We interpret this result to suggest
296 that radical oxidation—wherein electronic effects should contribute significantly to carbocation
297 stabilization—is irreversible and governs product distribution. Additionally, analysis of selectivity
298 outcomes with respect to computed C(sp^3)–H BDFEs across the ethylbenzene series indicates no
299 significant correlation between product selectivity and BDFE (**Figure 5E)**.[68] These findings are
300 most consistent with turnover-limiting HAT followed by an irreversible, product-determining
301 radical oxidation. Further studies are ongoing to probe additional mechanistic details.

302 Altogether, this work suggests that a HAT-ORPC strategy can provide a site-selective platform
303 for C(sp^3)–H functionalization. An advantage to this method is the utilization of phthalimide-
304 derived species as redox-active HAT reagents; these reagents are not only readily available, but
305 also are highly tunable. In this context, we questioned whether site-selectivity in the fluorination
306 of ibuprofen ethyl ester—a complex substrate possessing various C(sp^3)–H bonds—could be tuned
307 on the basis of the radical species used in HAT (**Figure 6A**). Under standard conditions with the
308 methyl radical precursor **1**, the fluorination of ibuprofen ethyl ester favored C(sp^3)–H
309 functionalization at the tertiary benzylic site over the secondary benzylic site (**38**, 2.4:1 rr) (**Figure**

6A). This site-selectivity is orthogonal to previously reported HAT-guided strategies (**Figure 6B**)[7,22,38] but consistent with our mechanistic studies that indicate a preference for tertiary C(sp^3)–H functionalization according to BDFE and radical oxidation potential considerations (**Figure 5C**). Furthermore, methyl radical is polarity matched to abstract a hydrogen atom proximal to an electron withdrawing group. By contrast, the prior art relies on electrophilic HAT mediators that are polarity mismatched to abstract a hydrogen atom proximal to an electron withdrawing group. As such, we hypothesized that employment of **3**, a precursor to the electrophilic methoxy radical, would afford distinct site-selectivity, favoring more electron-rich C(sp^3)–H sites. Indeed, we observed a reversal of site-selectivity in this case, wherein ibuprofen ethyl ester was fluorinated in 31% yield with a 5.3:1.5:1 rr favoring the secondary benzylic site (**62**). This example demonstrates the potential for this platform to engage readily available small molecule HAT reagents for tunable and predictable site-selective C(sp^3)–H functionalization.

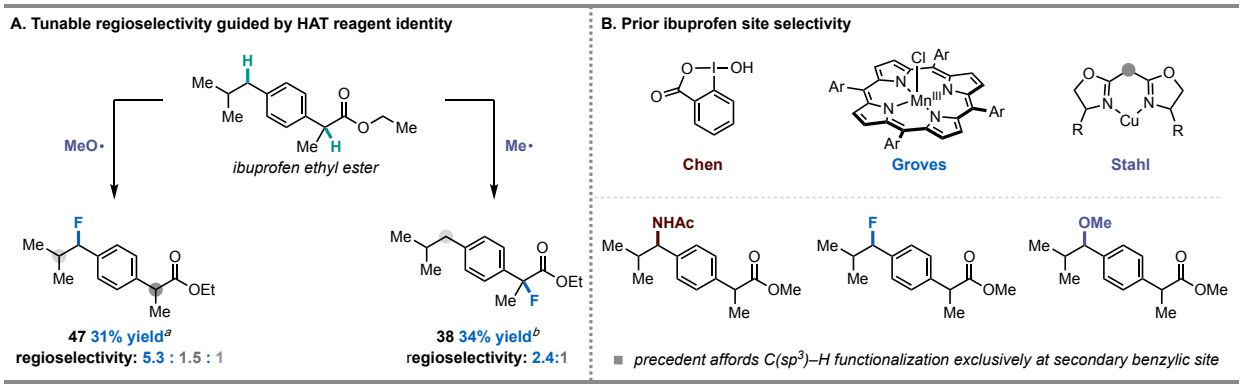

Figure 6. (A) Tunable selectivity for the C(sp^3)–H functionalization of ibuprofen demonstrating favorable secondary benzylic fluorination with methoxy radical (left) and favorable tertiary benzylic fluorination with methyl radical (right). (B) Previous examples of site-selectivity in the C(sp^3)–H functionalization of ibuprofen. [a] Reaction performed using abstractor **3** and standard reaction conditions described in **Figure 2.** [b] Reaction performed using abstractor **1** and standard reaction conditions described in **Figure 2**.

In conclusion, we have developed a photocatalytic method that employs widely available, low-cost nucleophiles and a readily accessible HAT precursor for C(sp^3)–H fluorination, chlorination, etherification, thioetherification, azidation, and carbon–carbon bond formation. Mechanistic

studies are consistent with methyl radical-mediated HAT and linear free-energy relationships suggest that radical oxidation influences site-selectivity. Furthermore, this approach was highly effective for the construction of multi-halogenated scaffolds and the late-stage functionalization of several bioactive molecules and pharmaceuticals with tunable regioselectivity.

References

1. Sladojevich, F., Arlow, S. I., Tang, P. & Ritter, T. Late-stage deoxyfluorination of alcohols with PhenoFluor. *J. Am. Chem. Soc.* **135**, 2470–3 (2013).

2. Yamaguchi, J., Yamaguchi, A. D. & Itami, K. C–H Bond Functionalization: Emerging Synthetic Tools for Natural Products and Pharmaceuticals. *Angew. Chem. Int. Ed.* **51**, 8960–9009 (2012).

3. Davies, H. M. L. & Morton, D. Recent Advances in C–H Functionalization. *J. Org. Chem.* **81**, 343–350 (2016).

4. Lee, B. J., DeGlopper, K. S. & Yoon, T. P. Site-Selective Alkoxylation of Benzylic C−H Bonds by Photoredox Catalysis. *Angew. Chem. Int. Ed.* **59**, 197–202 (2020).

5. Beatty, J. W. & Stephenson, C. R. J. Amine Functionalization via Oxidative Photoredox Catalysis: Methodology Development and Complex Molecule Synthesis. *Acc. Chem. Res.* **48**, 1474–84 (2015).

6. Guo, X., Zipse, H. & Mayr, H. Mechanisms of Hydride Abstractions by Quinones. *J. Am. Chem. Soc.* **136**, 13863–13873 (2014).

7. Li, G.-X., Morales-Rivera, C. A., Gao, F., Wang, Y., Gang, H., Liu, P. & Chen, C. A unified photoredox-catalysis strategy for C(sp^3)–H hydroxylation and amidation using hypervalent iodine. *Chem. Sci.* **8**, 7180–7185 (2017).

8. Capaldo, L. & Ravelli, D. Hydrogen Atom Transfer (HAT): A Versatile Strategy for Substrate Activation in Photocatalyzed Organic Synthesis. *Eur. J. Org. Chem.* **2017**, 2056–2071 (2017).

9. Pierre, J.-L. & Thomas, F. Homolytic C–H bond cleavage (H-atom transfer): chemistry for a paramount biological process. *CR. Chim.* **8**, 65–74 (2005).

10. Capaldo, L., Quadri, L. L. & Ravelli, D. Photocatalytic hydrogen atom transfer: the philosopher's stone for late-stage functionalization? *Green Chem.* **22**, 3376–3396 (2020).

11. Shaw, M. H., Twilton, J. & MacMillan, D. W. C. Photoredox Catalysis in Organic Chemistry. *J. Org. Chem.* **81**, 6898–6926 (2016).

12. González-Esguevillas, M., Miró, J., Jeffrey, J. L. & MacMillan, D. W. C. Photoredox-catalyzed deoxyfluorination of activated alcohols with Selectfluor®. *Tetrahedron* **75**, 4222–4227 (2019).

13. Bloom, S., Pitts, C. R., Miller, D. C., Haselton, N., Holl, M. G., Urheim, E., & Lectka, T. A Polycomponent Metal-Catalyzed Aliphatic, Allylic, and Benzylic Fluorination. *Angew. Chem. Int. Ed.* **51**, 10580–10583 (2012).

14. Ventre, S., Petronijevic, F. R. & MacMillan, D. W. C. Decarboxylative Fluorination of Aliphatic Carboxylic Acids via Photoredox Catalysis. *J. Am. Chem. Soc.* **137**, 5654–5657 (2015).

15. Proctor, R. S. J. & Phipps, R. J. Recent Advances in Minisci-Type Reactions. *Angew. Chem. Int. Ed.* **58**, 13666–13699 (2019).

16. Liang, T., Neumann, C. N. & Ritter, T. Introduction of fluorine and fluorine-containing functional groups. *Angew. Chem. Int. Ed.* **52**, 8214–64 (2013).

17. Caron, S. Where Does the Fluorine Come From? A Review on the Challenges Associated with the Synthesis of Organofluorine Compounds. *Org. Process Res. Dev.* **24**, 470–480 (2020).

18. Bafaluy, D., Georgieva, Z. & Muñiz, K. Iodine Catalysis for C(sp^3)–H Fluorination with a Nucleophilic Fluorine Source. *Angew. Chem. Int. Ed.* **59**, 14241–14245 (2020).

19. Nair, V., Suja, T. D. & Mohanan, K. A convenient protocol for C–H oxidation mediated by an azido radical culminating in Ritter-type amidation. *Tetrahedron Lett.* **46**, 3217–3219 (2005).

20. Bao, X., Wang, Q. & Zhu, J. Copper-catalyzed remote C(sp^3)–H azidation and oxidative trifluoromethylation of benzohydrazides. *Nat. Commun.* **10**, 769 (2019).

21. Le, C., Liang, Y., Evans, R. W., Li, X. & MacMillan, D. W. C. Selective sp^3 C–H alkylation via polarity-match-based cross-coupling. *Nature* **547**, 79–83 (2017).

22. Hu, H., Chen, S.-J., Mandal, M., Pratik, S. M., Buss, J. A., Krska, S. W., Cramer, C. J. & Stahl, S. S. Copper-catalysed benzylic C–H coupling with alcohols via radical relay enabled by redox buffering. *Nat. Catal.* **3**, 358–367 (2020).

23. Zhang, W., Wang, F., McCann, S. D., Wang, D., Chen, P., Stahl, S. S. & Liu, G. Enantioselective cyanation of benzylic C–H bonds via copper-catalyzed radical relay. *Science* **353**, 1014–1018 (2016).

24. Suh, S.-E., Chen, S.-J., Mandal, M., Guzei, I. A., Cramer, C. J. & Stahl, S. S. Site-Selective Copper-Catalyzed Azidation of Benzylic C–H Bonds. *J. Am. Chem. Soc.* **142**, 11388–11393 (2020).

25. Liu, W., Huang, X., Cheng, M.-J., Nielsen, R. J., Goddard, W. A. & Groves, J. T. Oxidative aliphatic C-H fluorination with fluoride ion catalyzed by a manganese porphyrin. *Science* **337**, 1322–5 (2012).

26. Huang, X., Bergsten, T. M. & Groves, J. T. Manganese-Catalyzed Late-Stage Aliphatic C–H Azidation. *J. Am. Chem. Soc.* **137**, 5300– 5303 (2015).

27. Liu, W. & Groves, J. T. Manganese Catalyzed C–H Halogenation. *Acc. Chem. Res.* **48**, 1727–1735 (2015).

28. Liu, W. & Groves, J. T. Manganese Porphyrins Catalyze Selective C−H Bond Halogenations. *J. Am. Chem. Soc.* **132**, 12847–12849 (2010).

29. Bower, J. K., Cypcar, A. D., Henriquez, B., Stieber, S. C. E. & Zhang, S. C(sp^3)–H Fluorination with a Copper(II)/(III) Redox Couple. *J. Am. Chem. Soc.* **142**, 8514-8521 (2020).

30. Webb, E. W., Park, J. B., Cole, E. L., Donnelly, D. J., Bonacorsi, S. J., Ewing, W. R. & Doyle, A. G. Nucleophilic (Radio)Fluorination of Redox-Active Esters via Radical-Polar Crossover Enabled by Photoredox Catalysis. *J. Am. Chem. Soc.* **142**, 9493-9500 (2020).

31. Shibutani, S., Kodo, T., Takeda, M., Kazunori, N., Tokunaga, N., Sasaki, Y. & Ohmiya, H. Organophotoredox-Catalyzed Decarboxylative C(sp^3)–O Bond Formation. *J. Am. Chem. Soc.* **142**, 1211–1216 (2020).

32. Hou, Z., Liu, D.-J., Xiong, P., Lai, X.-L., Song, J. & Xu, H.-C. Site-Selective Electrochemical Benzylic C−H Amination. *Angew. Chem. Int. Ed.* **59**, 1-6 (2020).

33. Wang, H., Liang, K., Xiong, W., Samanta, S., Li, W. & Lei, A. Electrochemical oxidation-induced etherification via C(sp^3)─H/O─H cross-coupling. *Sci. Adv.* **6**, 1-6 (2020).

34. O'Hagan, D. Understanding organofluorine chemistry. An introduction to the C–F bond. *Chem. Soc. Rev.* **37**, 308–319 (2007).

35. Szpera, R., Moseley, D. F. J., Smith, L. B., Sterling, A. J. & Gouverneur, V. The Fluorination of C−H Bonds: Developments and Perspectives. *Angew. Chem. Int. Ed.* **58**, 14824–14848 (2019).

36. McMurtrey, K. B., Racowski, J. M. & Sanford, M. S. Pd-Catalyzed C–H Fluorination with Nucleophilic Fluoride. *Org. Lett.* **14**, 4094–4097 (2012).

37. Braun, M.-G. & Doyle, A. G. Palladium-Catalyzed Allylic C–H Fluorination. *J. Am. Chem. Soc.* **135**, 12990–12993 (2013).

38. Huang, X., Liu, W., Ren, H., Neelamegam, R., Hooker, J. M. & Groves, J. T. Late Stage Benzylic C–H Fluorination with [18F]Fluoride for PET Imaging. *J. Am. Chem. Soc.* **136**, 6842–6845 (2014).

39. Cornella, J., Edwards, J. T., Qin, T., Kawamura, S., Wang, J., Pan, C.-M., Gianatassio, R., Schmidt, M., Eastgate, M. D. & Baran, P. S. Practical Ni-Catalyzed Aryl–Alkyl Cross-Coupling of Secondary Redox-Active Esters. *J. Am. Chem. Soc.* **138**, 2174–2177 (2016).

40. Blanksby, S. J. & Ellison, G. B. Bond Dissociation Energies of Organic Molecules. *Acc. Chem. Res.* **36**, 255–263 (2003).

41. In our examination of optimal reaction solvent we found pivalonitrile to be ideal for this transformation. Solvents possessing abstractable C–H bonds, such as acetonitrile or dichloromethane, resulted in competitive HAT from solvent and therefore fluorination in only moderate yield. Fluorination was also suppressed in the presence of aromatic solvents, due to competitive arene functionalization by methyl radical.

42. Syroeshkin, M. A., Krylov, I. B., Hughes, A. M., Alabugin, I. V., Nasybullina, D. V., Sharipov, M. Y., Gultyai, V. P. & Terent'ev, A. O. Electrochemical behavior of N-oxyphthalimides: Cascades initiating self-sustaining catalytic reductive *N—O* bond cleavage. *J. Phys. Org. Chem.* **30**, 1-15 (2017).

43. Mukherjee, S., Maji, B., Tlahuext-Aca, A. & Glorius, F. Visible-Light-Promoted Activation of Unactivated C(sp^3)–H Bonds and Their Selective Trifluoromethylthiolation. *J. Am. Chem. Soc.* **138**, 16200–16203 (2016).

44. Saha, B., Koshino, N. & Espenson, J. H. N -Hydroxyphthalimides and Metal Cocatalysts for the Autoxidation of p -Xylene to Terephthalic Acid. *J. Phys. Chem.* **108**, 425–431 (2004).

45. Smith, J. M., Qin, T., Merchant, R. R., Edwards, J. T., Malins, L. R., Liu, Z., Che, G., Shen, Z., Shaw, S. A., Eastgate, M. D. & Baran, P. S. Decarboxylative Alkynylation. *Angew. Chem. Int. Ed.* **56**, 11906–11910 (2017).

46. Teegardin, K., Day, J. I., Chan, J. & Weaver, J. Advances in Photocatalysis: A Microreview of Visible Light Mediated Ruthenium and Iridium Catalyzed Organic Transformations. *Org. Process Res. Dev.* **20**, 1156–1163 (2016).

47. Okada, K., Okamoto, K., Morita, N., Okubo, K. & Oda, M. Photosensitized decarboxylative Michael addition through N-(acyloxy)phthalimides via an electron-transfer mechanism. *J. Am. Chem. Soc.* **113**, 9401–9402 (1991).

48. Leung, J. C. T., Chatalova-Sazepin, C., West, J. G., Rueda-Becerril, M., Paquin, J.-F. & Sammis, G. M. Photo-fluorodecarboxylation of 2-Aryloxy and 2-Aryl Carboxylic Acids. *Angew. Chem. Int. Ed.* **51**, 10804–10807 (2012).

49. Huang, X., Liu, W., Hooker, J. M. & Groves, J. T. Targeted Fluorination with the Fluoride Ion by Manganese-Catalyzed Decarboxylation. *Angew. Chem. Int. Ed.* **54**, 5241–5245 (2015).

50. Applequist, D. E. & Kaplan, L. The Decarbonylation of Aliphatic and Bridgehead Aldehydes. *J. Am. Chem. Soc.* **87**, 2194–2200 (1965).

51. Nielsen, M. K., Ugaz, C. R., Li, W. & Doyle, A. G. PyFluor: A Low-Cost, Stable, and Selective Deoxyfluorination Reagent. *J. Am. Chem. Soc.* **137**, 9571–9574 (2015).

52. While pyridines are predisposed to Minisci-type reactivity in the presence of alkyl radicals we observed no methyl radical incorporation in either the substrate or resulting fluorinated product.

53. Sorlin, A. M., Usman, F. O., English, C. K. & Nguyen, H. M. Advances in Nucleophilic Allylic Fluorination. *ACS Catal.* **10**, 11980–12010 (2020).

54. Guo, R., Huang, J. & Zhao, X. Organoselenium-Catalyzed Oxidative Allylic Fluorination with Electrophilic N–F Reagent. *ACS Catal.* **8**, 926–930 (2018).

55. Hollingworth, C., Hazari, A., Hopkinson, M. N., Tredwell, M., Benedetto, E., Huiban, M., Gee, A. D., Brown, J. M. & Gouverneur, V. Palladium-Catalyzed Allylic Fluorination. *Angew. Chem. Int. Ed.* **50**, 2613–2617 (2011).

56. Zafrani, Y., Yeffet, D., Sod-Moriah, G., Berliner, A., Amir, D., Marciano, D., Gershonov, E. & Saphier, S. Difluoromethyl Bioisostere: Examining the "Lipophilic Hydrogen Bond Donor" Concept. *J. Med. Chem.* **60**, 797–804 (2017).

57. Middleton, W. J. New fluorinating reagents. Dialkylaminosulfur fluorides. *J. Org. Chem.* **40**, 574–578 (1975).

58. In the fluorination of diphenylmethane to fluorodiphenylmethane, 3% difluorination product **44** was observed under standard fluorination conditions.

59. In reactions with 1:1 stoichiometry of diphenylmethane to abstractor **1**, monofluorinated product **2** is observed in 17% yield and difluorinated product **44** is observed in 2% yield. We hypothesize that diminished yields of **2** and **44** are a result of unproductive side reactivity associated with the methyl radical, which may be mitigated when either diphenylmethane or fluorodiphenyl methane substrate concentrations are high.

60. Dantignana, V., Milan, M., Cussó, O., Company, A., Bietti, M. & Costas, M. Chemoselective Aliphatic C–H Bond Oxidation Enabled by Polarity Reversal. *ACS Cent. Sci.* **3**, 1350–1358 (2017).

61. *n*-Bu_4NCl can also be used in the presence of water and 15 mol % $Et_3N{\bullet}3HF$. See SI for details.

62. Rueping, M. & Nachtsheim, B. J. A review of new developments in the Friedel–Crafts alkylation – From green chemistry to asymmetric catalysis. *Beilstein J. Org. Chem.* **6**, 6 (2010).

63. We considered the possibility that nucleophilic addition in this context could proceed via nucleophilic substitution from the in situ generated benzylic fluoride, as per: Vasilopoulos, A., Golden, D. L., Buss, J. A. & Stahl, S. S. Copper-Catalyzed C–H Fluorination/Functionalization Sequence Enabling Benzylic C–H Cross Coupling with Diverse Nucleophiles. *Org. Lett.* **22**, 5753–5757 (2020). However, further experiments exploring this possibility indicated that triethylamine HF does not contribute to a sequential functionalization-substitution mechanism in the context of these nucleophiles. See SI for an extended discussion.

64. Huihui, K. M. M., Caputo, J. A., Melchor, Z., Olivares, A. M., Spiewak, A. M., Johnson, K. A., DiBenedetto, T. A., Kim, S., Ackerman, L. K. G. & Weix, D. J. Decarboxylative Cross-Electrophile Coupling of N-Hydroxyphthalimide Esters with Aryl Iodides. *J. Am. Chem. Soc.* **138**, 5016–5019 (2016).

65. Sherwood, T. C., Xiao, H.-Y., Bhaskar, R. G., Simmons, E. M., Zaretsky, S., Rauch, M. P., Knowles, R. R. & Dhar, T. G. M. Decarboxylative Intramolecular Arene Alkylation Using N -(Acyloxy)phthalimides, an Organic Photocatalyst, and Visible Light. *J. Org. Chem.* **84**, 8360–8379 (2019).

66. Salomon, M. Isotope Effects in Methyl Radical Abstraction Reactions. *Can. J. Chem.* **42**, 610–613 (1964). Large KIEs observed in this study are in accordance with KIEs observed in previous experimental and theoretical studies for methyl radical HAT.

67. Baik, M.-H., Newcomb, M., Friesner, R. A. & Lippard, S. J. Mechanistic Studies on the Hydroxylation of Methane by Methane Monooxygenase. *Chem. Rev.* **103**, 2385–2420 (2003).

68. BDFEs were computed according to: John, P. C. St., Guan, Y., Kim, Y., Kim, S. & Paton, R. S. Prediction of organic homolytic bond dissociation enthalpies at near chemical accuracy with sub-second computational cost. *Nat. Commun.* **11**, 2328 (2020). In our experience, different levels of theory give slightly different ordering of the compounds by BDFE. This is due to energetic differences that are small relative to the error associated with DFT. However, all levels of theory evaluated gave similarly poor correlations and do not affect the conclusions drawn.

Data Availability

Materials and methods, experimental procedures, mechanistic studies, characterization data, spectral data, and xyz files (in accompanying zip drive) associated with computational data are available in the Supplementary Information.

Acknowledgements. Financial support was generously provided by NSF (CHE-1565983). M. A. T.-S. wishes to thank Princeton's Presidential Postdoctoral Fellowship for funding. István Pelzer, Kenneth Conover, and John Eng are acknowledged for analytical aid. We thank Dr. Eric W. Webb for early intellectual and experimental contributions to the project.

Author Contributions. Authors I. N.-M. L. and M. A. T.-S. contributed equally.

Competing Interests. The authors declare no competing interests.

Additional information

Supplementary information is available in the online version of the paper.

Correspondence and requests for materials should be addressed to A. G. D.